Rare Metal Materials and Engineering
Volume 45, Issue 9, September 2016
Online English edition of the Chinese language journal

Available online at www.sciencedirect.com
ScienceDirect

Cite this article as: Rare Metal Materials and Engineering, 2016, 45(9): 2246-2252.

ARTICLE

Effect of Y Addition on Isothermal Oxidation Behavior of $Ti_{50}Ni_{50}$ Shape Memory Alloy at 700 °C

Xu Jiawen[1], Liu Ailian[1], Wang Shuhua[1], Zhou Yuebo[1], Zhang He[1], Zhou Chang-hai[1], Cai Wei[2]

[1] Heilongjiang University of Science and Technology, Harbin 150022, China; [2] Harbin Institute of Technology, Harbin 150001, China

Abstract: The effect of Y addition on the microstructure and isothermal oxidation behaviour of an equal-atomic Ti-Ni shape memory alloy at 700 ℃ in air was investigated. The results show that the grains of the Ti-Ni alloy are evidently refined with Y addition. The oxidation rate significantly declines with the addition of 0.5 at%Y and 1.0 at%Y because the fast outward diffusion of Ti is inhibited by the segregated Y ions. However, the oxidation rate increases with 5.0 at%Y addition since the formation of oxide along the NiY phase breaks the continuity of the TiO_2 scale.

Key words: Ti-Ni SMAs; rare earth Y; isothermal oxidation; microstructure

Near equal-atomic Ti-Ni shape memory alloys (SMAs) are technologically important materials because of their outstanding shape memory effect (SME) and superelasticity [1]. Up to now the application of Ti-Ni SMAs has been spread to aerospace, aviation, medical field and other fields. Cold work can be applied to Ti-Ni alloys, which will result in work hardening rapidly. In addition, continuous deformation needs annealing. Hot working at 500~800 ℃ (in B2 phase state) in air is usually required to obtain a designed shape. Thus, oxidation of Ti-Ni alloys inevitably occurs during the annealing or the hot working process. There are few related researches on the oxidation behaviour of Ti-Ni SMAs reported [2-5].

According to the researches on the oxidation behaviour of ferrous and non-ferrous alloys, the addition of rare earth elements can prevent the oxide scale spallation and decrease the oxidation rate[6-8]. Liu et al [9-11] reported that the addition of Y, Ce, Dy and Gd have evident influences on martensitic transformation when they were added to Ti-Ni alloys. However, there is no report about the oxidation of $Ti_{50}Ni_{50}$ alloy with rare earth element Y addition. The aim of this paper is to study the effect of Y addition on the oxidation behavior of $Ti_{50}Ni_{50}$ alloy, which will be of benefit to its application.

1 Experiment

The experimental alloys were prepared by a non-consumable arc-melting furnace under an argon atmosphere using a water-cooled copper crucible. Firstly the binary alloy with a nominal composition of $Ti_{50}Ni_{50}$ was prepared by melting raw materials of 99.97 wt% sponge Ti and 99.7 wt% electrolytic Ni. After the ingot was cut into four parts, Y (99.95 wt%) was added to one part of them to prepare the ternary Ti-Ni-Y alloys with a series of nominal compositions of $Ti_{49.75}Ni_{49.75}Y_{0.5}$, $Ti_{49.5}Ni_{49.5}Y_1$, and $Ti_{47.5}Ni_{47.5}Y_5$. Hereafter, the experimental alloys were denoted as Y0, Y0.5, Y1 and Y5, respectively. During the arc melting process, the ingots were remelted at least six times and were flipped over after each melting step in order to ensure homogeneity.

The oxidation samples with a size of 10 mm×15 mm×2 mm were spark-cut from the ingots and solution treated at 900 ℃ for 1 h in the vacuum quartz capsules followed by quenching into water with breaking the capsules. Then they were conventionally ground on series of SiC abrasive papers from 500# to 2000# and mechanically polished using diamond polishing paste (average particle size: 2.5 μm). Subsequently,

Received date: September 23, 2015
Foundation item: National Natural Science Foundation of China (51201062, 51371078, 51501058)
Corresponding author: Liu Ailian, Associate Professor, College of Materials Science and Engineering, Heilongjiang University of Science and Technology, Harbin 150022, P. R. China, Tel: 0086-451-88036521, E-mail: liuailian@yeah.net

the samples were cleaned in acetone. Finally, the samples were dried in hot air. Before oxidation the samples were hung in the alumina crucibles and the total weight of the sample and the crucibles were measured using an electronic balance with 0.1 mg sensitivity.

The oxidation experiments of the Ti-Ni-Y alloys were carried out by interrupted oxidation. The interrupted oxidation tests were conducted in static air in the muffle furnace at 700 ℃ for 20 h. The alumina crucibles with samples were put into a furnace where the temperature had already been elevated to the test temperature. They were taken out from the furnace after holding for 1, 3, 5, 8, 10, 12, 15 and 20 h at 700 ℃, and then the samples with the crucibles were weighed when cooled down to room temperature in the air. The oxidation kinetics was evaluated by analyzing mass-gain data as a function of time.

The composition and phases of Ti-Ni-Y alloys before and after oxidation were investigated using Camscan MX2600FE type scanning electron microscopy (SEM) equipped with an energy dispersive spectroscopy (EDS) and a D/Max-2500 pc type X-ray diffractometer (XRD). In order to observe the morphology of the cross-section, a layer of electroless Ni-plating was plated on the surface of the oxidised specimens to prevent the spallation of the scales during the process of the sample preparation.

2 Results and Discussion

2.1 Microstructure of Ti-Ni-Y alloy

Fig.1 shows the optical microstructures of Ti-Ni alloys with and without Y addition. It is seen that the addition of Y refines the grains of the Ti-Ni alloy, because the formed Y-enriched particles not only promote the nucleation of new crystals during casting but also suppress the growth of Ti-Ni grains during heat-treatment process. These published results were reported in the Ti-Ni-Dy[10] or Ce[11] to binary Ti-Ni alloy.

In order to observe the microstructure and the distribution of rare earth element Y in the Ti-Ni-Y alloy, the back scattering electron images observation was carried out and the results are shown in Fig.2. It can be seen that in the Ti-Ni binary alloy, there are no second phases which is shown in Fig.2a. However, there are second phases dispersed along the grain boundaries and inside the grains (shown in Fig.2b, 2c and 2d), which is different from that of Ti-Ni alloys. Moreover, the fraction of second phase, the white phase in Fig.2, increases with the increase of Y content. The EDS analysis shows that the gray area in the Ti-Ni-Y alloy has a similar composition to the Ti-Ni alloy. However, the white phase is enriched in Y and the ratio of Ni:Y is nearly 1. The results suggest that the white phase may be NiY intermetallic phase, which is further confirmed by the XRD characterization shown in Fig.3.

From Fig.3, it can be seen that besides the characteristic peaks corresponding to NiY at 33.12°, 34.73° and 41.22°, several diffraction peaks can be indexed as characteristic peaks of Ti-Ni martensite, which indicate that Ti-Ni-Y alloys are also in martensite state at room temperature.

2.2 Isothermal oxidation

Fig.4 shows the oxidation kinetics curves of Ti-Ni shape memory alloys with and without Y additions in air at 700 ℃ for 20 h. No spallation occurs for any of the alloys during oxidation and the cooling process. From Fig.4a, it can be found that Y0.5 and Y1 exhibit an apparently lower mass gain than Y0 and Y5 in the short transient oxidation stage (the first 5 h), especially the latter. In this stage, a continuous scale is expected to thermally grow. After this period, the oxidation rate of Y0.5 and Y1 remains so low that no significant mass gain occurs. However, a significant mass gain occurs for

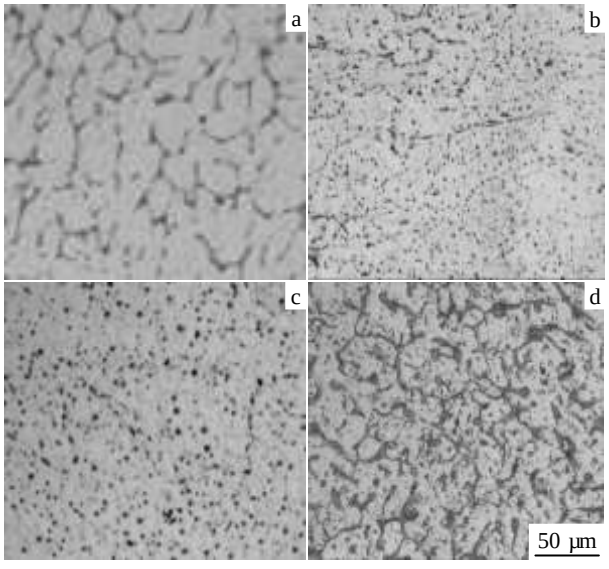

Fig.1 Optical microstructures of different TiNi alloys: (a) Y0, (b) Y0.5, (c) Y1, and (d) Y5

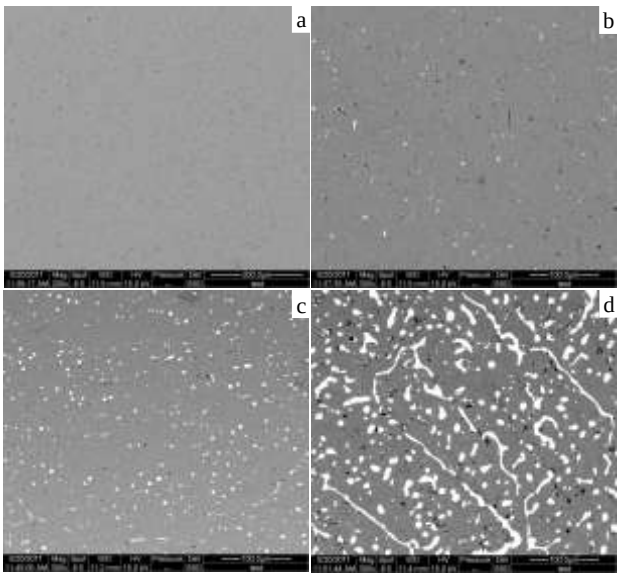

Fig.2 Back scattered electronic microstructures of different TiNi alloys: (a) Y0, (b) Y0.5, (c) Y1, and (d) Y5

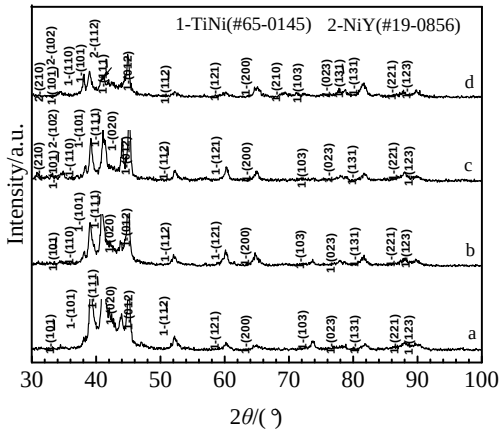

Fig.3 XRD patterns of different Ti-Ni-Y alloys (a- Y0, b- Y0.5, c- Y1, and d- Y5)

Y0 and Y5, especially the latter. The corresponding parabolic rate constant is 0.89×10^{-10}, 0.58×10^{-10}, 0.35×10^{-10} and 6.69×10^{-10} g^2/cm^4s for Y0, Y0.5, Y1 and Y5, respectively, as indicated in Fig.4a. It is seen clearly that the oxidation rate of Y0.5 and Y1 are lower than that of Y0, especially the latter. This is true that the oxidation rate of Y5 is higher than that of Y0. The addition of a small amount of Y (0.5 at% and 1.0 at%) can improve the oxidation resistance of Ti-Ni alloys, while more amount of Y (5.0 at%) deteriorates the oxidation resistance. In the present work, Y1 alloy exhibits the best oxidation resistance in all alloys, which can be further confirmed from the cross-sectional morphologies of oxide scale.

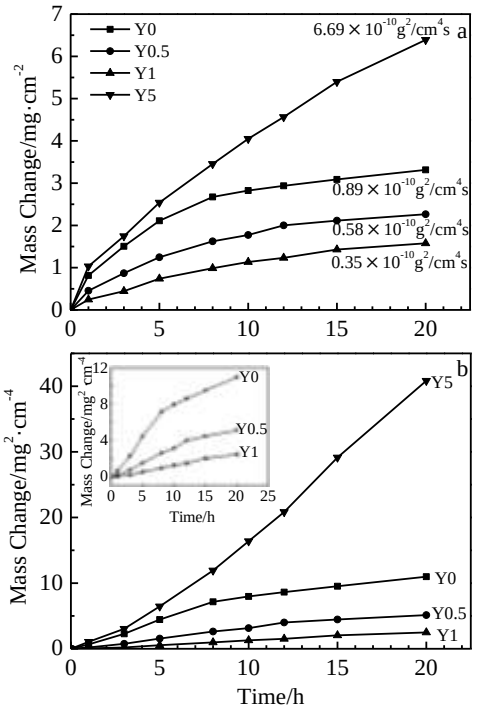

Fig.4 Kinetics of isothermal oxidation of different TiNi alloys in air at 700 ℃: (a) liner and (b) parabolic plot

After being oxidized at 700 ℃ for 20 h, Ti-Ni alloys with and without Y addition were further identified by XRD and the results are presented in Fig.5. The results show that a mixture of TiO_2 (rutile) and minor Ti-NiO_3 is formed on Y0, while the addition of 0.5 at% Y and 1.0 at%Y dramatically decreases the peak intensity of Ti-NiO_3 with the appearance of Y_2O_3 phase peak at a very low peak intensity. When the Y content reaches 5.0 at%, the peak intensity both of the Ti-NiO_3 and Y_2O_3 phase increases significantly.

To clarify the difference in the oxidation performance of Ti-Ni alloys with and without Y addition, surface and cross-sectional morphologies of the scales were investigated by the SEM method as shown in Fig.6 and Fig.7. Fig.6 shows the surface morphologies of the oxide scales formed on Ti-Ni-Y alloys exposed at 700 ℃ for 20 h. It is clear that the morphologies of the oxide scales formed on different Ti-Ni alloys are very similar. However, the oxide grain size gradually decreases with the increasing of Y content.

In order to verify the oxidation mechanism of Ti-Ni-Y alloys, the elemental profiles of the cross-section were also conducted by EDS, as shown in Fig.7. It can be seen that the black oxide scale on all alloys exhibits both a high Ti and O content. The bright phases in the mixture layer on Y0 exhibits a high Ni content, as seen in Fig.7a. Fig.7d shows a different element distribution in the bright phase area for Y5. The bright phases in one area (area 1 in Fig.7d) are Ni-rich and Ti-poor. However, another area poor in Ti and Ni and rich in Y and O can be observed (area 2 in Fig.7d). Combining these with the XRD results in Fig.5, we can identify both the TiO_2 outer layer and Ni_3Ti degradation zone, as seen in Fig.7. For Y0, the bright phases in the mixed inner layer are Ni and the black phase is TiO_2. Thus, the mixed inner layer is TiO_2 oxide scale with Ni dispersion. However, for Y5, the bright phase in area 1 and area 2 is Ni and Y_2O_3, respectively. The above results indicate that the scale structure formed during the high temperature oxidation changes with the increase of the Y

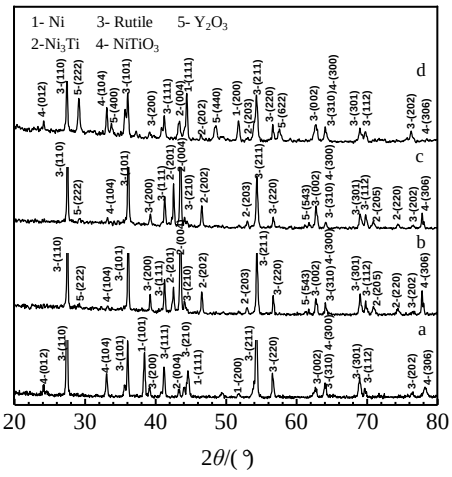

Fig.5 XRD patterns of scale formed on different TiNi alloys after 20 h oxidation at 700 ℃ in air (a- Y0, b- Y0.5, c- Y1 and d- Y5)

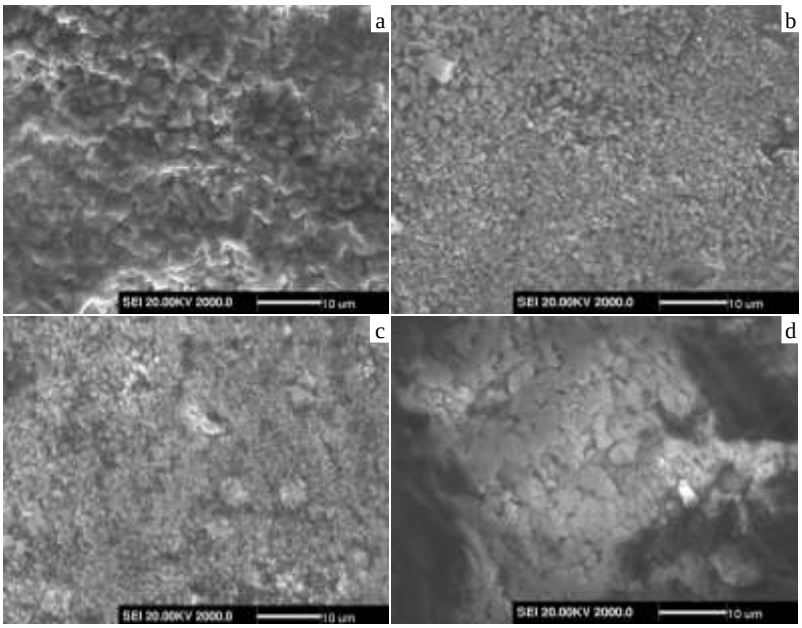

Fig.6 Surface morphologies of the scale formed on different TiNi alloys after 20 h oxidation at 700 ℃ in air: (a) Y0, (b) Y0.5, (c) Y1, and (d) Y5

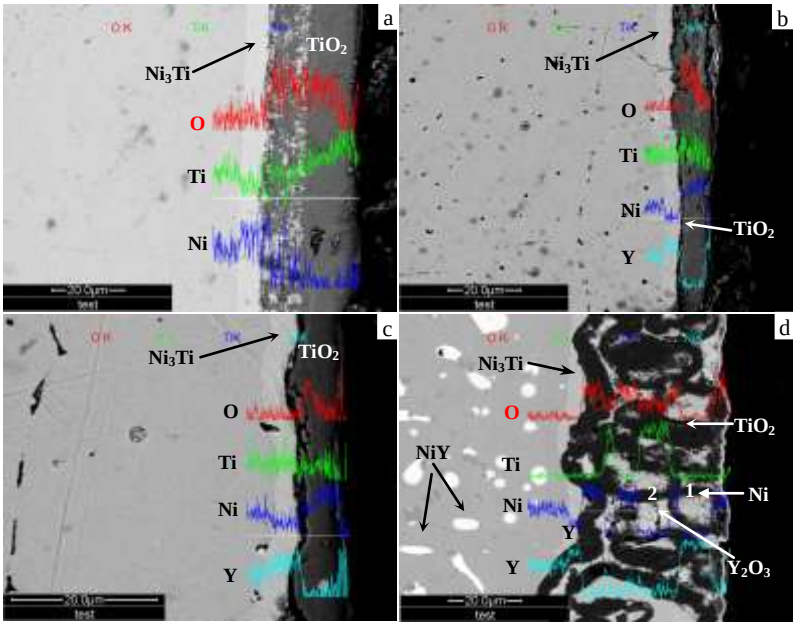

Fig.7 Cross-sectional SEM images and elemental depth profiles on different TiNi alloys after 20 h oxidation at 700 ℃ in air: (a) Y0, (b) Y0.5, (c) Y1, and (d) Y5

content. For the pure Ti-Ni alloy, a double layer scale structure, a TiO_2 outer layer and a (TiO_2 +Ni) mixture inner layer are formed. However, a single pure TiO_2 oxide scale is formed on Y0.5 and Y1. A further increase in the Y content will result in the formation of a netlike TiO_2 scale, in which large area of Ni and Y_2O_3 phases disperses. One should note that we refer to Ni as Ni (Ti) due to the dissolution of Ti again.

Fig.7 shows the cross-section of the specimens after oxidation at 700 ℃. It can be seen that the morphology of the cross section of oxidized Ti-Ni-Y alloys is different with Y content change. From Fig.7a, it can be seen that the scale formed on the Ti-Ni alloy without Y addition shows a three-layer structure consisting of a purer outer blacker layer (TiO_2 layer), a mixture inner layer (TiO_2/Ni layer) and a pure brighter inner layer (Ni_3Ti layer). The total scale thickness is about 27 μm. Large voids are observed in the outer TiO_2 layer

near the interface between the outer layer and the mixture inner layer. On the other hand, the inner layer contains many small voids and/or some uniformly distributed pores, especially near the inner/metal interface. However, for both the Y0.5 and Y1 alloys, the mixture of the inner layer disappears and the cross section contains an outer TiO_2 layer and an inner Ni_3Ti layer. The thickness of scale gradually decreases as seen in Fig.7b and Fig.7c. In the ternary Ti-Ni-Y alloys, there are numerous small pores in which the NiY phase is located, as indicated from the arrows in Fig.7d. On this basis, one may conclude that the pores formed due to the pull-out of part of the Y-rich phases during polishing, are the relatively loose interface between the Y-rich phase and the metal. A similar result was also reported in the Ni deposited with dispersion of the CeO_2 nano-particles[12]. However, when Y content reaches 5.0 at%, the oxide scale exhibits a netlike structure. Also the area of bright phase is significantly enlarged, as seen in Fig.7d.

3 Discussion

According to XRD patterns of scale formed on the Ti-Ni-Y alloys as shown in Fig.5, Ti-NiO_3 phase forms after the oxidation of Ti-Ni-Y alloys at 700 ℃. The formation of Ti-NiO_3 is due to the reaction of NiO and TiO_2, especially for Y0 and Y5 which have a higher oxidation rate. This indicates the oxidation of Ni. The above results illustrate that the addition of 0.5 at%Y and 1.0 at%Y significantly hinders the formation of Ti-NiO_3 and leads to the formation of pure TiO_2 with a lower oxidation rate. Fig.5a and Fig.5d show that the higher oxidation rate of Y0 and Y5 are caused by the faster degradation of Ti-Ni alloys and quickly converts the Ti-Ni phase in the detection depth scope into the Ni and Ni_3Ti phase. From the Ti-Ni binary phase diagram [13], Ti can be solid-soluted in Ni lattice space. Thus, the authors of this paper suggest that these "Ni" peaks do not represent pure Ni metal, but rather a phase of Ni containing solid-soluted Ti atoms. We refer to this phase as Ni (Ti). In contrast, Y0.5 and Y1 still remain in the Ni_3Ti phase structure in the detection depth scope. This suggests that the addition of 0.5 at%Y and 1.0 at%Y significantly block the outward diffusion of Ti to TiO_2 oxide scale.

For oxidation of the Ti-Ni alloy, there is only the minor TiO_2-NiO oxide formed in the scale although Ti-Ni contains a large amount of Ni. This may reflect the difference in the oxygen affinity between Ti and Ni, i.e., Ti is easily oxidized while Ni is more difficult to oxidize [14]. Therefore, at the onset of oxidation, Ti is oxidized first to form the TiO_2 (rutile) nuclei while the remained Ni unchanges. As the rutile nuclei grow, both in the vertical and horizontal directions, a rutile layer is formed. During this process, titanium diffuses outwardly while oxygen diffuses inwardly. Since the diffusivity of Ti in the rutile is faster than that of oxygen, the outward diffusion of Ti controls the oxidation progress. Thus a Ti degradation zone is formed beneath the scale [2,3]. Then, a Ni (Ti) and a Ni_3Ti layer beneath the scale developed. Once the TiO_2 oxide layer reaches a certain thickness, the inward diffusion of oxygen through the outer scale begins to take effect on the scale growth. When oxygen diffuses into the Ni (Ti) phase, the less noble component Ti is oxidized to form TiO_2 particles due to low oxygen pressure there. This results in a mixture layer of Ni (Ti) and TiO_2 being formed [2,3]. At the same time, a minor amount of NiO may form in the inner layer at the low oxygen pressure [4]. The reaction of NiO with TiO_2 causes the formation of the Ti-NiO_3 spinal. The outward diffusion of Ti and inward diffusion of Ni causes so many small voids in the inner layer and at the inner/metal interface[2,3], especially the latter. In contrast, the coarsening and sintering of the TiO_2 grains in the outer layer produces excessive vacancies, which are then condensed in some available sites (such as at GB triple junctions) to form large voids[15,16]. However, it is not possible to condense near the scale/gas interface because the outward diffusion of Ti to form TiO_2 particles may quickly fills these voids. Thus, large voids mainly form near the inner/outer interface, as seen in Fig.7a.

In general, the additions of RE or RE oxides, such as Y, Ce, and La, which have a high affinity for oxygen, can enhance the selective oxidation and decrease the growth rate of NiO, Cr_2O_3 and Al_2O_3. This phenomenon was first reported in 1937 [17] and is referred to as the “reactive element effect (REE)”. Various theories to elucidate the REE have been put forward but still are in dispute because the mechanism may differ for different oxide/RE systems[18-20]. In the present work, one note is that the addition of Y refines the grain of the Ti-Ni alloy. It seems that the growth rate of TiO_2 on Y0.5 and Y1 should be at least as fast as that on the Ti-Ni alloy[20]. Moreover, since the growth of the TiO_2 scale is mainly controlled by the outward diffusion of Ti in the oxide scale along the oxide grain boundaries[2-4], the fine-grained TiO_2 scale formed on Y0.5 and Y1 should grow even faster than pure Ti-Ni alloy. This is because of an increase in the number of grain boundaries per unit volume in the scale [21,22]. However, it is significant that the oxidation rate is reduced. The aforementioned results suggest that the addition of an appropriate amount of Y should significantly block the outward diffusion of Ti along grain boundaries.

At the onset of oxidation, TiO_2 and Y_2O_3 nucleate at the grain boundaries of the Ti-Ni alloy and Y-rich particles on the alloy surface form, respectively. TiO_2 on the scale grows rapidly and engulfs the Y_2O_3 oxide particles, so a continuous external TiO_2 scale without Y_2O_3 particles is developed by healing the TiO_2 nuclei through their lateral growth during transient oxidation. After the transient stage of oxidation an oxygen potential gradient is established in the metal-scale-gas system. It is proposed that Y begins to take effect on the scale according to the "dynamic-segregation theory" proposed by Pint[20]. Y ions from the added Y or its oxides by dissolution

first segregate into the metal/scale interface and then to the gas/scale interface through the scale-grain boundaries[23-27]. When the concentration of Y ions at the scale grain boundaries reaches a critical value, the segregation-diffusion of Y ions prevents the outward Ti diffusion and it results in scale growth which is controlled primarily by inward oxygen diffusion. Previous works [28-33] found that the predominant outward diffusion of Ni along NiO grain boundaries was inhibited effectively by the segregated La, Y and Ce ions at the grain boundaries. This led to a reduction of the oxidation rate and the formation of a fine crystal structure. During the oxidation process, more Y_2O_3 particles incorporated into TiO_2 oxide dissolve to produce Y ions segregated to the oxide grain boundaries and then inhibiting the Y concentration at the grain boundaries was reduced with the increasing oxidation time. Moreover, the pinning[33] and "solute-drag" effect[20] of Y_2O_3 at the oxide grain boundaries give rise to the formation of fine oxide grains, as shown in Fig.6. This provides an indirect but credible piece of evidence that the segregated Y ions at the grain boundaries occur and the outward diffusion of Ti is hindered, to some extent, by segregated Y ions. Moreover, from Fig.7d, it can be found that the scale growth on Y5 is mainly controlled by the inward diffusion of O. The results also provide to the reader indirect and credible evidence that the addition of Y changes the oxidation mechanism from the outward Ti diffusion in the absence of RE into dominant inward oxygen diffusion.

According to the analysis above mentioned, it can be found that the addition of Y blocks the outward diffusion of Ti and changes the oxidation growth mechanism. This causes a reduction in the oxidation rate because the inward oxygen diffusion is much lower than the outward Ti diffusion. At the same time, the voiding kinetics at the scale/metal interface and within the scale[33] and the Ti degradation of the Ti-Ni alloy are decreased, which in turn retards the formation of the mixture layer of Ni (Ti) and TiO_2, as shown in Fig.7b and Fig.7c. In this case, a thinner and denser TiO_2 external scale forms. However, the increase in Y content to 5.0 at% has a detrimental effect because the Y-rich phase precipitated in the Ti-Ni alloy becomes a second phase with a fast oxidation rate. This results in an oxide penetration into the alloy along this phase [25, 33, 34]. The formation of Y_2O_3 oxides breaks the continuity of the protective TiO_2 scale. Thus a new TiO_2 layer forms beneath the original one. During this progress, the fast degradation of Ti also causes the formation of Ni solution. As a result, a netlike TiO_2 scale with Ni and Y_2O_3 phase dispersion forms, as seen in Fig.7d.

4 Conclusions

1) The microstructures of $Ti_{50}Ni_{50}$ alloy obviously changes with Y addition and Y-rich NiY phase formation.

2) The addition of 5.0 at% Y significantly increases the oxidation rate because the formation of TiO_2 nodules along the NiY phase breaks the continuity of the protective TiO_2 scale.

3) The addition of 0.5 at% and 1.0 at% Y significantly reduces the oxidation rate because the fast outward diffusion of Ti is inhibited by the segregated Y ions. This is especially true for the latter.

References

1 Miyazaki S, Otsuka K, Suzuki Y. *Scripta Metallurgica*[J], 1981, 15: 287

2 Chu C L, Wu S K, Yen Y C. *Materials Science and Engineering* A[J], 1996, 216:193

3 Xu C H, Ma X Q, Shi S Q *et al*. *Materials Science and Engineering A*[J], 2004, 371: 45

4 Okada M, Souwa M, Kasai T *et al*. *Applied Surface Science*[J], 2011, 257: 4257

5 Firstov G S, Vitchev R G, Kumar H *et al*. *Biomaterial*[J], 2002, 23: 4863

6 Xu G H, Wang G F, Zhang K F. *Transactions of the Nonferrous Metals Society of China*[J], 2011, 21(S2): 362

7 Paúl A, Elmrabet S, Odriozola J A. *Journal of Alloys and Compounds*[J], 2001, 323-324: 70

8 Cueff R, Buscail H, Caudron E *et al*. *Corrosion Science*[J], 2003, 45: 1815

9 Liu A L, Sui J H, Lei Y C *et al*. *Journal of Materials. Science*[J], 2007, 42: 5791

10 Liu A L, Gao Z Y, Gao L *et al*. *Journal of Alloys and Compounds*[J], 2007, 437: 339

11 Liu A L. *Thesis for Doctorate*[D]. Harbin: Harbin Institute of Technology, 2007 (in Chinese)

12 Peng X, Yan J, Xu C *et al*. *Metallurgical and Materials Transactions A: Physical Metallurgy and Materials Science*[J], 2008, 39: 119

13 Thaddeus B. *Binary Alloy Phase Diagrams*[M]. Geauga County, Ohio: ASM International, 1992: 2753

14 Lee H G. *Chemical Thermodynamics for Metals and Materials* [M]. London: Imperial College Press, 1999: 275

15 Li J G, Ye Y P, Shen L Y *et al*. *Materials Science and Engineering A*[J], 2005, 390: 265

16 Li D, Chen S O, Shao W Q *et al*. *Materials Letter*[J], 2008, 62: 849

17 Pfeil L B. *UK Patent*, 459848[P], 1937

18 Moon D P. *Materials Science and Technology*[J], 1989, 5: 754

19 Pieraggi B, Rapp R A. *Journal of the Electrochemical Society*[J], 1993, 140: 2844

20 Pint B A. *Oxidation of Metals*[J], 1996, 45: 1

21 Atkonson H V, Taylor R I, Goode P D. *Oxidation of Metals*[J], 1979, 13: 519

22 Atkonson H V. *Oxidation of Metals*[J], 1987, 28: 353

23 Yan J B, Gao Y M, Liang L *et al*. *Corrosion Science*[J], 2011, 53: 329

24 Zhang P, Guo X P. *Corrosion Science*[J], 2013, 71: 10

25 Zhou Y B, Sun J F, Wang S C *et al*. *Corrosion Science*[J], 2012, 63: 351

26 Zhu L J, Zhu S L, Wang F H *et al*. *Corrosion Science*[J], 2014, 80: 393

s

27 Zhang H, Peng X, Wang F H. *Surface and Coatings Technology*[J], 2012, 206: 2354
28 Peng X, Ping D H, Li T F *et al*. *Journal of the Electrochemical Society*[J], 1995, 145: 389
29 Peng X, Li T, Wu W. *Oxidation Metals*[J], 1999, 51: 291
30 Peng X, Li T, Wu W *et al*. *Materials Science and Engineering A*[J], 2001, 298: 100
31 Qu N S, Zhu D, Chan K C. *Scripta Materialia*[J], 2006, 54: 1421
32 Xue Y J, Liu H B, Lan M M *et al*. *Surface and Coatings Technology*[J], 2010, 204: 3539
33 Hindam H M, Whiiile D P. *Journal of the Electrochemical Society*[J], 1982, 129: 1147
34 Wang W, Yu P, Wang F H *et al*. *Surface and Coatings Technology*[J], 2007, 201: 7425

稀土 Y 对 $Ti_{50}Ni_{50}$ 形状记忆合金 700 ℃下恒温氧化行为的影响

徐家文[1]，刘爱莲[1]，王淑花[1]，周月波[1]，张　鹤[1]，周长海[1]，蔡　伟[2]

(1. 黑龙江科技大学，黑龙江 哈尔滨 150022)

(2. 哈尔滨工业大学，黑龙江 哈尔滨 150001)

摘　要：研究了添加稀土元素 Y 对等原子比 Ti-Ni 形状记忆合金显微组织和 700 ℃恒温氧化行为的影响。结果表明，随 Y 的加入 Ti-Ni 合金的晶粒得到明显细化。当 Y 含量为 0.5at%和 1.0at%时，Y 的加入显著降低了 Ti-Ni 合金的氧化速率，这是由于少量的 Y 抑制了 Ti 元素向外层的迅速扩散。然而当 Y 含量为 5.0at%时，含 Y 的 Ti-Ni 合金的氧化速率增大，原因是沿 NiY 相形成的氧化物破坏了 TiO_2 氧化膜的连续性。

关键词：Ti-Ni 形状记忆合金；稀土 Y；恒温氧化；显微组织

作者简介：徐家文，男，1975 年生，副教授，黑龙江科技大学材料学院，黑龙江 哈尔滨 150022，电话：0451-88036521，E-mail: xujiawen@sina.com